Available online at www.sciencedirect.com
SCIENCE DIRECT®
Journal of Solid State Chemistry 178 (2005) 1508–1512
JOURNAL OF SOLID STATE CHEMISTRY
www.elsevier.com/locate/jssc

Synthesis and properties of the $Co_7Se_{8-x}S_x$ and $Ni_7Se_{8-x}S_x$ solid solutions

Virginia Lea Miller[a,*], Wei-li Lee[b], Gavin Lawes[c], Nai-Phuan Ong[b], Robert J. Cava[a]

[a]*Department of Chemistry, Frick Chemical Laboratory, Princeton University, Washington Road, Princeton, NJ 08544, USA*
[b]*Department of Physics, Princeton University, Princeton, NJ 08544, USA*
[c]*Los Alamos National Laboratory, Los Alamos, NM 87544, USA*

Received 2 September 2004; received in revised form 29 October 2004; accepted 2 November 2004
Available online 23 March 2005

Abstract

We report the synthesis and elementary properties of the $Co_7Se_{8-x}S_x$ ($x = 0-8$) and $Ni_7Se_{8-x}S_x$ ($x = 0-7$) solid solutions. Both systems form a NiAs-type structure with metal vacancies. In general, the lattice parameters decrease with increasing x, but in the $Ni_7Se_{8-x}S_x$ system c increases on going from $x = 5$ to 7. Magnetic susceptibility measurements show that all samples exhibit temperature-independent paramagnetism from 25–250 K. Samples within the $Co_7Se_{8-x}S_x$ system, as well as Ni_7Se_8 and Ni_7SeS_7, were found to be poor metals with resistivities of ~0.20 and ~0.06 mΩ cm at 300 K, respectively. The Sommerfeld constant (γ) was determined from specific heat measurements to be ~13 $mJ/mol_{Co}K^2$ and ~7 $mJ/mol_{Ni}K^2$ for $Co_7Se_{8-x}S_x$ and $Ni_7Se_{8-x}S_x$, respectively.

Keywords: $Co_7Se_{8-x}S_x$; $Ni_7Se_{8-x}S_x$; Cobalt and nickel chalcogenides; Magnetic properties

1. Introduction

Unlike binary oxides of the 3*d* transition metals, which are typically antiferromagnetic insulators, binary transition metal chalcogenides can have widely varying magnetic and electronic properties. Chromium, for example, forms several stable sulfides and selenides, most of which display either antiferromagnetism or ferrimagnetism [1]. With the exception of Cr_2S_3, Cr_7Se_8 and Cr_3Se_4, the chromium sulfides and selenides are metallic conductors [1]. Manganese sulfide (MnS) and selenides (MnSe and $MnSe_2$) are antiferromagnetic semiconductors whereas many iron sulfides and selenides exhibit room temperature ferromagnetism and metallic conductivity [2–6]. Further along the 3*d* series, the selenides and sulfides of copper are paramagnetic [7,8]. Thus, there is a transition from magnetic to nonmagnetic properties as the 3*d* transition metal progresses from chromium to copper. Since cobalt and nickel are situated at the boundary between magnetic and nonmagnetic behavior, it is of interest to study the properties of these metal chalcogenides to determine where this transition occurs, and whether any unexpected behavior can be found at the crossover point.

Binary systems containing a 3*d* transition metal and a chalcogenide often form the NiAs structure, i.e. FeSe, CoSe and NiSe [1,9]. This structure can allow for variable composition with vacancies on either the metal or chalcogenide site. For example, Fe_7Se_8 has a defect NiAs structure with ordered vacancies on the Fe site. The observed ferrimagnetism (T_c~483 K) of this compound arises from the uncompensated moments due to the ordering of the Fe vacancies [10]. Within each metal layer, the spins on the Fe atoms are aligned ferromagnetically but are aligned antiferromagnetically between adjacent layers. This magnetic arrangement is also present in Fe_7S_8, which has a T_c~600 K [11]. A study

*Corresponding author. Fax: +1 609 258 6746.
E-mail address: vmiller@princeton.edu (V.L. Miller).

0022-4596/$ - see front matter © 2004 Elsevier Inc. All rights reserved.
doi:10.1016/j.jssc.2004.11.013

of the $Fe_7Se_{8-x}S_x$ system revealed that long-range ordering is hindered for intermediate composition ($1.2 < x < 6.8$) but increases as the end members are approached [11].

Both CoSe and NiSe form defect NiAs-type structures with variable compositions, i.e. $Co_{1-x}Se$ and $Ni_{1-x}Se$ [1,9]. CoSe exhibits Curie–Weiss type magnetism and NiSe is weakly paramagnetic [12]. Co_7Se_8 is also reported to have a defect NiAs-type structure with $a = 3.604$ Å and $c = 5.276$ Å and it exhibits Pauli paramagnetism [13]. As for many simple binary chalcogenides, the sulfides and selenides have the same structure type. Both CoS and NiS are also reported to form a NiAs-type structure [1,9]. However, no physical properties have been reported for Ni_7S_8, Co_7S_8 or the $Ni_7Se_{8-x}S_x$ and $Co_7Se_{8-x}S_x$ solid solutions. Therefore, the focus of this study was to synthesize these two solid solutions and to characterize their physical properties; increasing the sulfur content is expected to favor more localized electronic behavior, such as seen in $NiS_{2-x}Se_x$ [14]. In addition, the increase in sulfur concentration could cause an increase in the metal–metal orbital overlap, which may cause a change in the electronic and/or magnetic properties of these solid solutions.

2. Experimental

Polycrystalline powder samples of $Co_7Se_{8-x}S_x$ ($x = 0, 1, 3, 5, 7, 8$) and $Ni_7Se_{8-x}S_x$ ($x = 0, 1, 2, 3, 4, 5, 6, 7$) were synthesized from the pure elements. Stoichiometric amounts of Co (99.8%) or Ni (99.7%), Se (99.99%) and S (99.999%) were placed in evacuated quartz tubes at 400 °C for 12 h. The temperature was then increased 100 °C every 24 h until the final temperature reached 800 °C. The samples were heated at 800 °C for several days and then annealed at 400 °C for one week to facilitate vacancy ordering. Attempts to prepare Ni_7S_8 using this technique were unsuccessful.

Single crystals of needle-like Ni_7Se_8 and Ni_7SeS_7 were grown using vapor transport. The pre-reacted polycrystalline powders of the desired compounds were sealed in quartz tubes with ~10 wt% iodine, and the tubes were then placed in a temperature gradient of 900 °C/800 °C for one week. Small single crystals formed at the cooler end of the gradient.

Powder X-ray diffraction (Cu$K\alpha$ radiation) was used to determine the phase purity of all samples. A Quantum Design PPMS was used to obtain magnetic susceptibility measurements of the $Ni_7Se_{8-x}S_x$ samples from 5 to 250 K in a field of 10 kOe. For the $Co_7Se_{8-x}S_x$ samples, however, initial magnetic measurements indicated the presence of a trace amount of Co metal impurity (see inset of Fig. 2). As a result, the susceptibility of these compounds was determined by calculating the difference in magnetization between applied fields of 20 and 40 kOe ($\chi = \Delta M/\Delta H$). This procedure was performed in the temperature range 5–275 K, with a temperature step of 10 K, using a SQUID magnetometer (Quantum Design). This technique has been previously used to measure the intrinsic susceptibility of $MgCNi_3$ samples, which typically contain a trace amount of ferromagnetic Ni metal impurity [15].

For the $Co_7Se_{8-x}S_x$ solid solution, heat capacity measurements were performed on sintered polycrystalline samples using a standard semi-adiabatic heat pulse technique at zero applied field. Members of the $Ni_7Se_{8-x}S_x$ solid solution decomposed into a

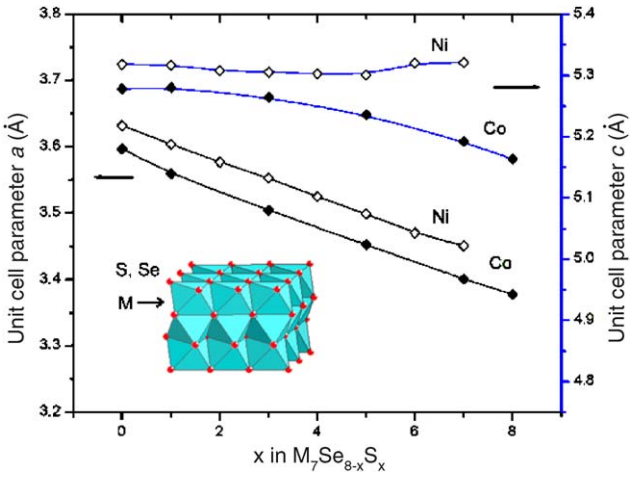

Fig. 1. Hexagonal unit cell paramaters a and c (in Å) versus x for $Co_7Se_{8-x}S_x$ (closed diamonds) and $Ni_7Se_{8-x}S_x$ (open diamonds). The inset shows the NiAs crystal structure. The red spheres represent the S, Se atoms and the M atoms are inside the blue polyhedra.

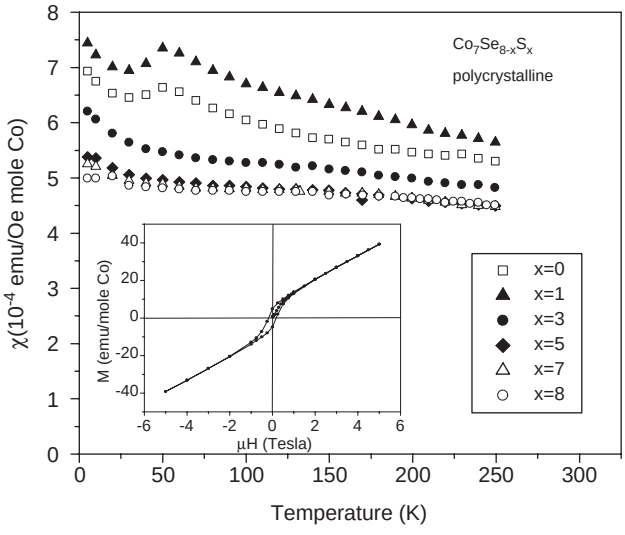

Fig. 2. Temperature dependent magnetic susceptibility measurements ($\chi = \Delta M/\Delta H$) for samples of $Co_7Se_{8-x}S_x$. The inset is a plot of magnetization versus applied magnetic field at 100 K for Co_7Se_7S.

multi-phase product when pressed into pellets and sintered. As a result, for the specific heat measurements on this system, the as-prepared powder sample was cold sintered into a hard pellet with Ag powder in a 1:1 ratio to facilitate thermal equilibration. The contribution to the heat capacity from Ag powder was subtracted from the total value.

Resistivity measurements of the polycrystalline $Co_7Se_{8-x}S_x$ samples and single crystal Ni_7Se_8 and Ni_7SeS_7 samples were performed using four-probe geometry and a conventional lock-in amplifier technique. The resistivity of the single crystals were measured along the *c*-axis.

3. Results and discussion

All samples were found to be single phase by powder X-ray diffraction and to crystallize in a hexagonal unit cell with space group $P6_3/mmc$ (#194). The crystallographic cell parameters were determined from a least-squares fit to 8–10 X-ray reflections between 10° and 90° 2θ. Fig. 1 illustrates the changes in the unit cell parameters as a function of x in $M_7Se_{8-x}S_x$. For both systems, the a parameter decreases as x increases. For the $Co_7Se_{8-x}S_x$ compounds, a decreases from 3.597(3)Å for Co_7Se_8 to 3.378(1)Å for Co_7S_8. The c parameter also decreases as x increases. In the Ni system, a decreases from 3.632(1)Å for Ni_7Se_8 to 3.451(1)Å for Ni_7SeS_7. This is expected given the fact that the ionic radius of S^{2-} (1.84 Å) is smaller than that of Se^{2-} (1.98 Å); so the substitution of S for Se should cause a decrease in the size of the unit cell [16]. However, in the $Ni_7Se_{8-x}S_x$ system the c parameter decreases from 5.318(1)Å for Ni_7Se_8 to 5.301(1)Å for $Ni_7Se_3S_5$ and then increases from 5.301(1)Å for $Ni_7Se_3S_5$ to 5.320(1)Å for Ni_7SeS_7. The reason for this has yet to be determined.

Figs. 2 and 3 show the temperature dependence of magnetic susceptibility (χ) in the range of 5–250 K for the $Co_7Se_{8-x}S_x$ and $Ni_7Se_{8-x}S_x$ samples, respectively. All measured samples exhibit temperature-independent paramagnetism from 25 to 250 K. For the $Co_7Se_{8-x}S_x$ samples, the magnetic susceptibility decreases and becomes more temperature-independent as x increases from 1 to 8. The small peak that occurs around 50 K for the Co_7Se_8 and Co_7Se_7S samples does not correspond to Co_3O_4 ($T_N = 40$ K) or any other identifiable impurity. This suggests that this peak is intrinsic to these two samples. The inset of Fig. 2 is a plot of magnetization versus applied field for Co_7Se_7S, which clearly shows the presence of Co metal impurity. A plot of magnetization versus applied field for Co yielded a saturation magnetization of 9000 emu/mol Co, which indicates a 1 part per thousand impurity of Co metal. This trace amount of Co metal impurity was not detectable using X-ray diffraction. In the Ni system, the magnetic susceptibility is temperature-independent from 25 to

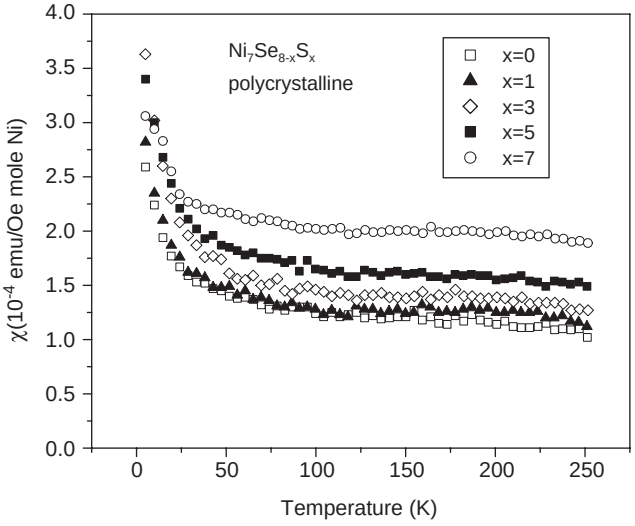

Fig. 3. Temperature dependent magnetic susceptibility measurements for samples of $Ni_7Se_{8-x}S_x$.

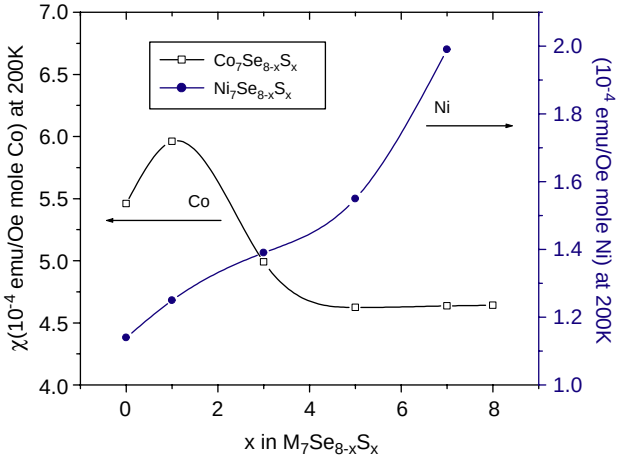

Fig. 4. Magnetic susceptibility at 200 K versus x for $Co_7Se_{8-x}S_x$ (open squares) and $Ni_7Se_{8-x}S_x$ (closed circles).

250 K and increases slightly as x varies from 0 to 7. The increase in χ at temperatures below 25 K is possibly the result of a Curie–Weiss paramagnetic impurity. A spin 1 impurity (Ni^{2+}) of ~4% was calculated from a Curie–Weiss fit of the low temperature (5–25 K) data. The magnetic susceptibility at 200 K versus x for $Co_7Se_{8-x}S_x$ and $Ni_7Se_{8-x}S_x$ is plotted in Fig. 4. In the $Co_7Se_{8-x}S_x$ solid solution, the magnetic susceptibility decreases as x ranges from 1 to 3 and then levels off at higher values of x. The reverse happens in the $Ni_7Se_{8-x}S_x$ system where the magnetic susceptibility continues to increases with increasing values of x. Overall, the magnetic susceptibility is higher for the $Co_7Se_{8-x}S_x$ samples than it is for the $Ni_7Se_{8-x}S_x$ samples.

Figs. 5 and 6 show the heat capacity data for the $Co_7Se_{8-x}S_x$ and $Ni_7Se_{8-x}S_x$ solid solutions, respectively.

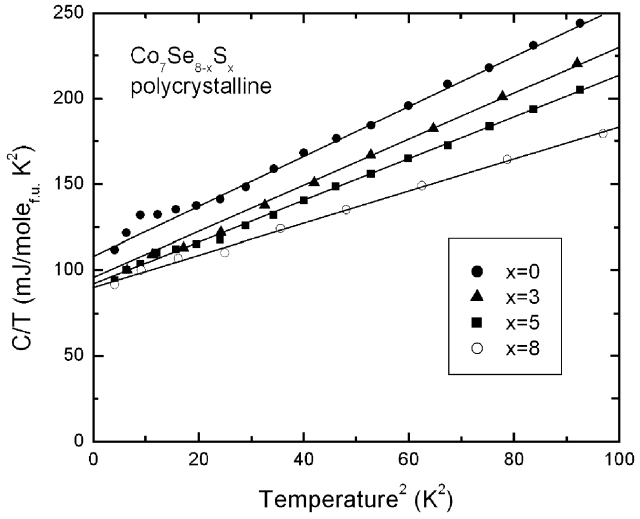

Fig. 5. Specific heat measurements of select polycrystalline $Co_7Se_{8-x}S_x$ samples.

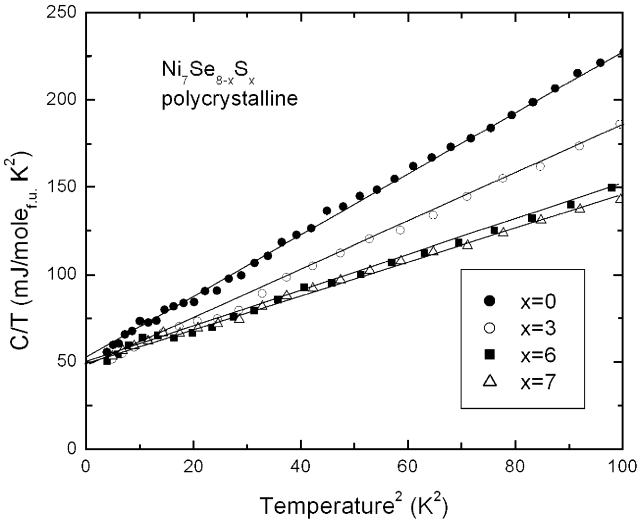

Fig. 6. Specific heat measurements of select polycrystalline $Ni_7Se_{8-x}S_x$ samples.

In both sets of data, the slope and y-intercept ($C/T = \gamma + \beta T^2$) show little variation with changes in x. The Debye temperature was found to range from 185 K for Co_7Se_8 to 220 K for Co_7S_8 and from 254 K for Ni_7Se_8 to 314 K for Ni_7SeS_7. For the $Co_7Se_{8-x}S_x$ samples, the Sommerfeld constant (γ) was determined to be $\sim$13 mJ/mol$_{Co}$K^2. Likewise, a value of $\sim$7 mJ/mol$_{Ni}$K^2 was found for the $Ni_7Se_{8-x}S_x$ samples. These values of gamma are low compared with other compounds on the boundary of magnetic versus nonmagnetic behavior. For example, Sr_2RuO_4 has a Sommerfeld constant of 40 mJ/mol$_{Ru}$K^2, which indicates the presence of strongly correlated electrons [17]. In a conventional metal, the contribution of the conduction electrons to the specific heat is γT, where $\gamma = (\pi^2/3)D(E_F)k_B^2$. As a result, gamma provides an experimental estimate of the density of states $D(E_F)$ at the Fermi level. So the heat capacity data presented in Figs. 5 and 6 support the claim that the $Co_7Se_{8-x}S_x$ samples have a higher $D(E_F)$ than the $Ni_7Se_{8-x}S_x$ samples.

A rough estimate of the Wilson ratio, $R_w = (\pi^2 k_B^2/3\mu_B^2)(\chi/\gamma)$, was also determined for members of these two solid solutions [18]. The value of the magnetic susceptibility measured at 200 K was used in this calculation. For the $Co_7Se_{8-x}S_x$ system, R_w was calculated to be approximately 2.5 for all samples. However, in the $Ni_7Se_{8-x}S_x$ series R_w was found to increase systematically from approximately 1.2 for $x = 0$ to 2.0 for $x = 7$. The Wilson ratio is expected to be between 1 and 2 for electronic systems that are conventional ($R_w = 1$) or those that show spin fluctuation enhancement of the susceptibility ($R_w = 2$). For the Ni system, increasing spin fluctuations are clearly implied as x increases. For the Co system, R_w is quite high. The reason for this has yet to be determined although impurities within the samples may have affected the value of the magnetic susceptibility.

The electrical resistivity of the $Co_7Se_{8-x}S_x$ and $Ni_7Se_{8-x}S_x$ samples is illustrated in Figs. 7 and 8, respectively. Both sets of data show a small change of resistivity with temperature. However, in both the

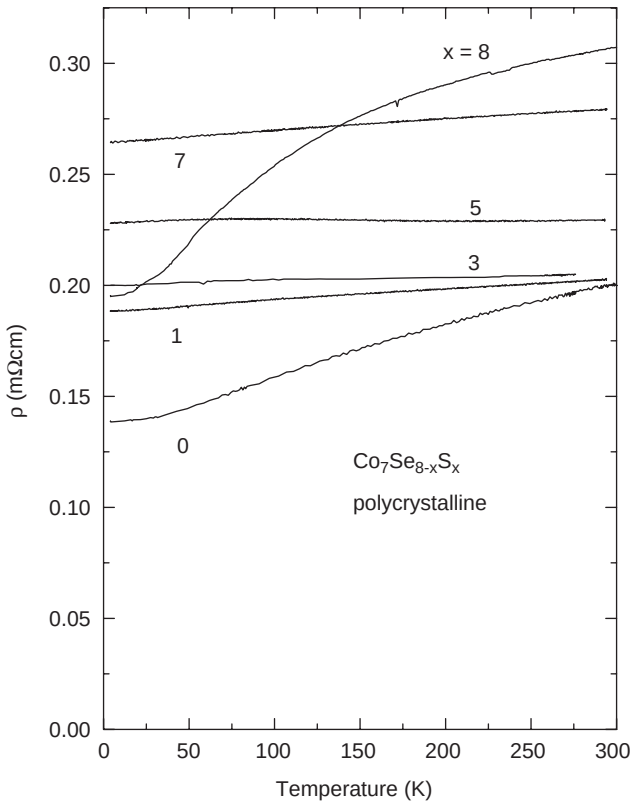

Fig. 7. Resistivity versus temperature for polycrystalline samples of $Co_7Se_{8-x}S_x$.

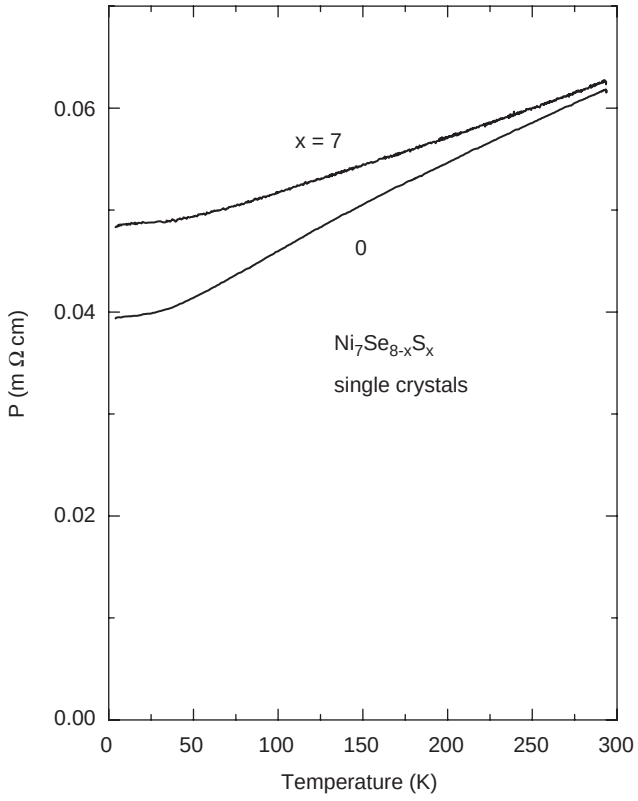

Fig. 8. Resistivity versus temperature for single crystals of Ni_7Se_8 and Ni_7SeS_7.

systems $\delta\rho/\delta\underline{T}>0$, which indicates that all samples are poor metals. It is interesting to note that in the $Co_7Se_{8-x}S_x$ system, samples of intermediate composition show very little variation in resistivity as the temperature is increased.

4. Conclusions

In this study, we report the synthesis and magnetic and electronic properties of the $Co_7Se_{8-x}S_x$ and $Ni_7Se_{8-x}S_x$ solid solutions. Members of these two systems form the NiAs-type structure with vacancies on the metal site. Magnetic measurements show that all samples exhibit temperature-independent paramagnetism from 25 to 250 K. Both the magnetic susceptibility and specific heat data support the claim that the $Co_7Se_{8-x}S_x$ compounds have a higher density of states at the Fermi level than the $Ni_7Se_{8-x}S_x$ compounds. Moreover, resistivity measurements of both polycrystalline pellets and single crystals reveal that the compounds are poor metals. These results show that there is an abrupt cross-over from magnetic to nonmagnetic behavior in $M_7Se_{8-x}S_x$ between Fe and Co. Although our estimate of the Wilson ratio in the $Co_7Se_{8-x}S_x$ system is anomalous, there is little indication in the other data for unusual magnetic or electronic states at the magnetic–nonmagnetic crossover in the 3*d* transition metal-chalcogenide systems.

Acknowledgments

This work was supported by the National Science Foundation (MRSEC Program) through the Princeton Center for Complex Materials (DMR 0213706).

References

[1] T.B. Massalski (Ed.), Binary Alloy Phase Diagrams, vol. 2, second ed., ASM International, 1990.
[2] J. Bousquet, M. Diot, M. Roubin, CR Acad. Sci. (Paris) 267C (1968) 861.
[3] F.M.A. Carpay, Philips Res. Rep. 10 (Suppl.) (1968).
[4] H. van der Heide, C.F. van Bruggen, C. Haas, Mater. Res. Bull. 18 (1983) 1515.
[5] N.R. Akhmedov, N.Z. Dzhalilov, D. Sh. Abdinov Izv. Akad. Nauk SSSR Neorg. Mater. 9 (1973) 1429.
[6] S. Takele, G.R. Hearne, J. Phys.: Condens. Matter 13 (2001) 10077.
[7] Z. Vucic, Z. Ogorelec, J. Magn. Magn. Mater. 15-18 (1980) 1175.
[8] R.A. Munson, W. DeSorbo, J.S. Kouvel, J. Chem. Phys. 47 (1967) 1769.
[9] T.B. Massalski (Ed.), Binary Alloy Phase Diagrams, vol. 3, second ed., ASM International, 1990.
[10] M. Kawaminami, A. Okazaki, J. Phys. Soc. Jpn. 29 (1970) 649.
[11] T. Ericsson, O. Amcoff, P. Nordblad, Eur. J. Mineral. 9 (1997) 1131.
[12] M.M. Abd-el Aal, J. Mater. Sci. 23 (1988) 3490.
[13] H. Ikeda, M. Shirai, N. Suzuki, K. Motizuki, J. Magn. Magn. Mater. 140–144 (1995) 159.
[14] G. Krill, P. Panissod, M.F. Lapierre, F. Gautier, C. Robert, G. Czjzek, J. Fink, H. Schmidt, R. Kuentzler, J. Phys. Colloq. 4 (1976) 23.
[15] M.A. Hayward, M.K. Haas, A.P. Ramirez, T. He, K.A. Regan, N. Rogado, K. Inumaru, R.J. Cava, Solid State Commun. 119 (2001) 491.
[16] R.D. Shannon, Acta Crystallogr. A 32 (1976) 751.
[17] S. Nishizaki, Y. Maeno, S. Farner, S. Ikeda, T. Fujita, Physica C 282–287 (1997) 1413.
[18] Y. Maeno, K. Yoshida, H. Hashimoto, S. Nishizaki, S. Ikeda, M. Nohara, T. Fujita, A.P. Mackenzie, N.E. Hussey, J.G. Bednorz, F. Lichtenberg, J. Phys. Soc. Japan 66 (1997) 1405.